

Supplemental Figures

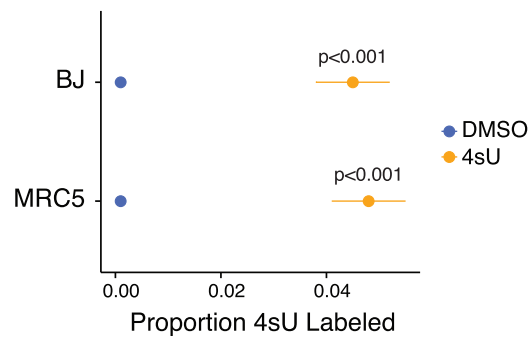


Figure S1. Labeling of RNA from Stromal Fibroblasts with 4sU, Related to Figure 1

Proportion of 4sU-labeled RNA in indicated fibroblasts after 24 hr compared to total RNA (n = 3). Error bars are SEM of biological replicates.

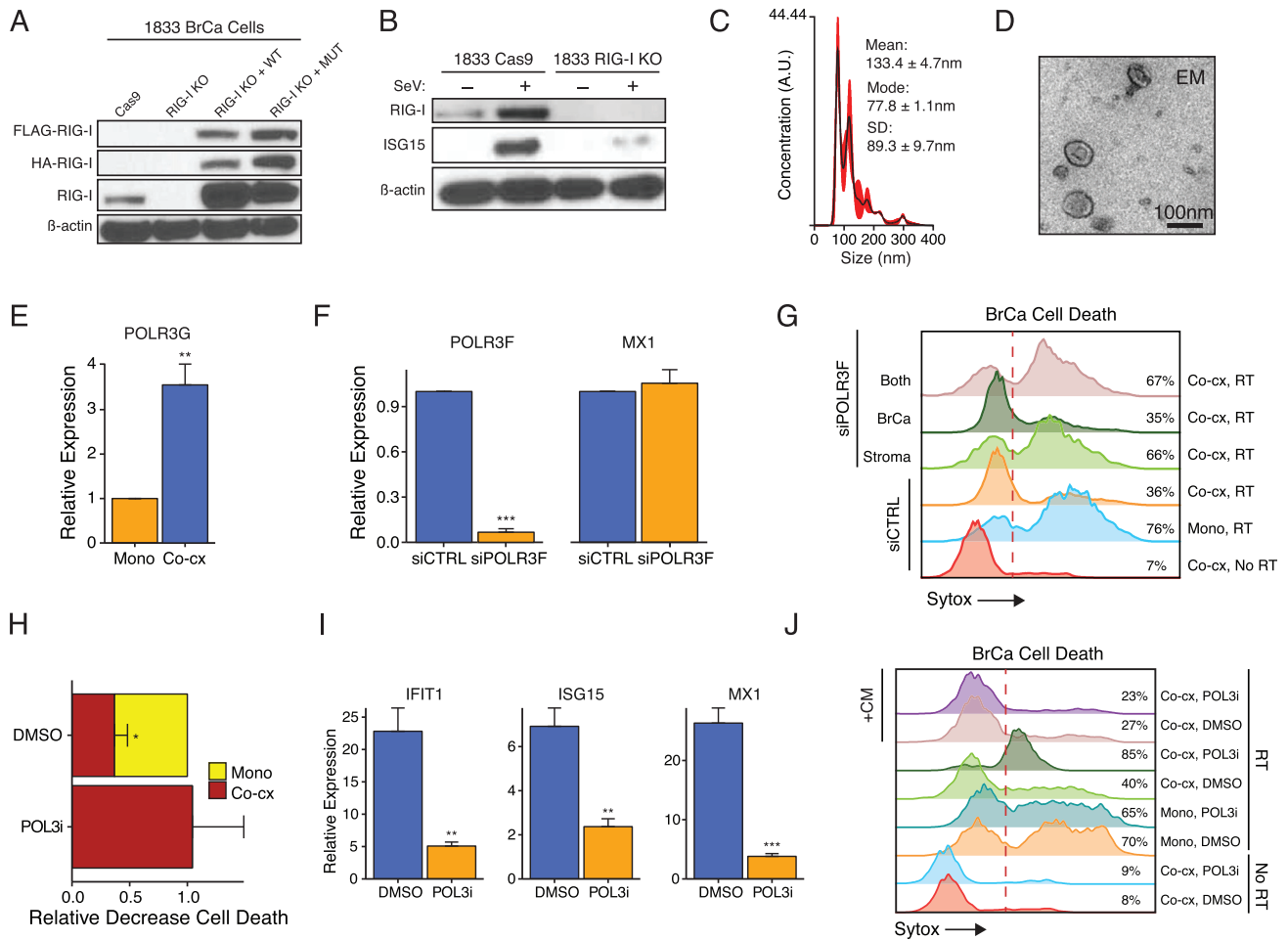


Figure S2. Breast Cancer RIG-I Signaling Is Regulated by 5'-Triphosphate ExoRNA and Stromal POL3, Related to Figure 2

(A) Immunoblot for RIG-I or epitope tag from Cas9 control (WT), RIG-I knockout (KO), and RIG-I KO 1833 cells restored with either wild-type (KO + WT) or RIG-I^{K858/861A} 5'ppp binding mutant (KO + MUT). (B) Immunoblot for RIG-I from 1833 ISG-R breast cancer cells with or without RIG-I knockout. RIG-I pathway activation was stimulated by Sendai virus (SeV) and assessed by ISG15 induction. (C) Nanosight analysis of exosome size and quantity or (D) electron microscopy negative staining from a representative exosome purification. (E) Expression of *POLR3G* in sorted MRC5 fibroblast after co-culture with ISG-R 1833 breast cancer cells. Gene expression values are relative to MRC5 cells in mono-culture ($n = 3$). (F) Expression of *POLR3F* after siRNA knockdown in MRC5 cells ($n = 3$). *MX1* was additionally examined as a specificity control. (G) Representative flow cytometry of live/dead fluorescence dye (Sytox) uptake by 1833 cells 4 days after 10 Gy RT. 1833 cells were grown either in mono-culture (Mono) or in co-culture with MRC5 cells (Co-cx) after control (siCTRL) or siRNA knockdown of *POLR3F* (siPOLR3F) in 1833 (BrCa), MRC5 (Stroma), or both cell types (Both). (H) Relative cell death of 1833 cells in mono-culture (Mono) or co-culture with MRC5 cells (Co-cx) 4 days after 10 Gy RT ($n = 3$). Cells were grown in the presence of DMSO or POL3 inhibitor (Pol3i). (I) ISG expression in sorted 1833 cells after co-culture with MRC5 cells in the presence of DMSO or POL3i. Gene expression values are relative to 1833 cells in mono-culture ($n = 7$). (J) Representative flow cytometry of live/dead fluorescence dye (Sytox) uptake by 1833 cells treated with or without RT. 1833 cells were grown in mono-culture (Mono) or co-culture with MRC5 cells (Co-cx) in the presence of DMSO or POL3i and with (+CM) or without rescue using ISG-R co-culture CM. Error bars are SEM of biological replicates and ** $p < 0.01$, *** $p < 0.001$.

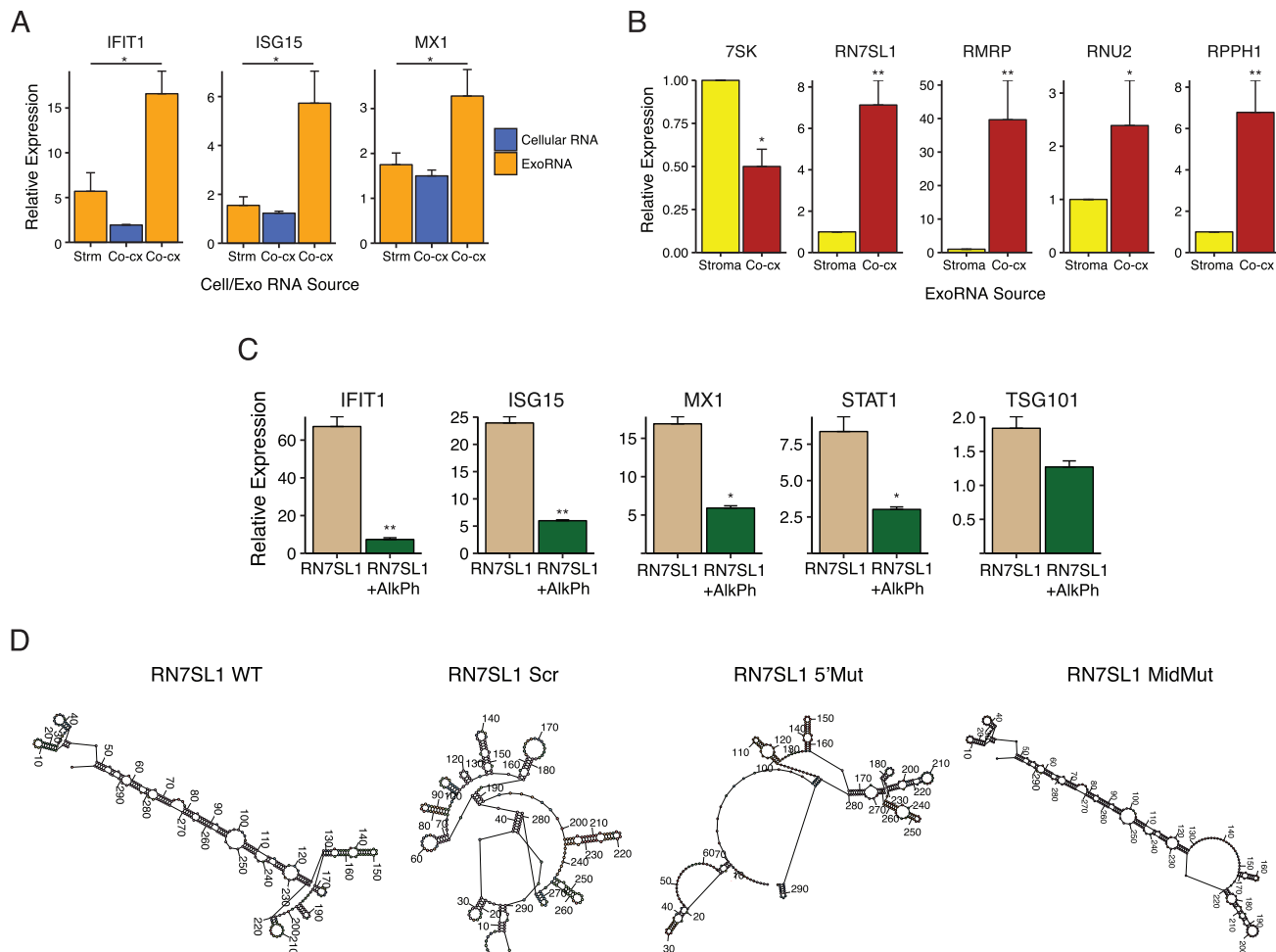


Figure S3. *RN7SL1* ExoRNA Is Transferred to Breast Cancer Cells to Activate RIG-I through Distinct Structural Features, Related to Figure 3
 (A) ISG expression in 1833 cells after transfection of exoRNA or cellular RNA from MRC5 mono-culture (Strm) or co-culture of 1833 and MRC5 cells (Co-cx) ($n = 3$). Values are relative to mock transfection. (B) Relative expression of transcripts identified by 5' ppp-seq in exosomes from MRC5 mono-culture (Stroma) or MRC5 and 1833 co-culture (Co-cx). Values are relative to exoRNA from MRC5 mono-culture ($n = 3$). (C) ISG expression in 1833 breast cancer cells after transfection of in vitro transcribed *RN7SL1* RNA or *RN7SL1* RNA treated with alkaline phosphatase (+AlkPh) ($n = 3$). *TSG101* is a non-ISG not expected to change. Values are relative to mock control. (D) Predicted RNA secondary structures of the *RN7SL1* and *RN7SL1* structural mutants. Error bars are SEM of biological replicates and * $p < 0.05$, ** $p < 0.01$.

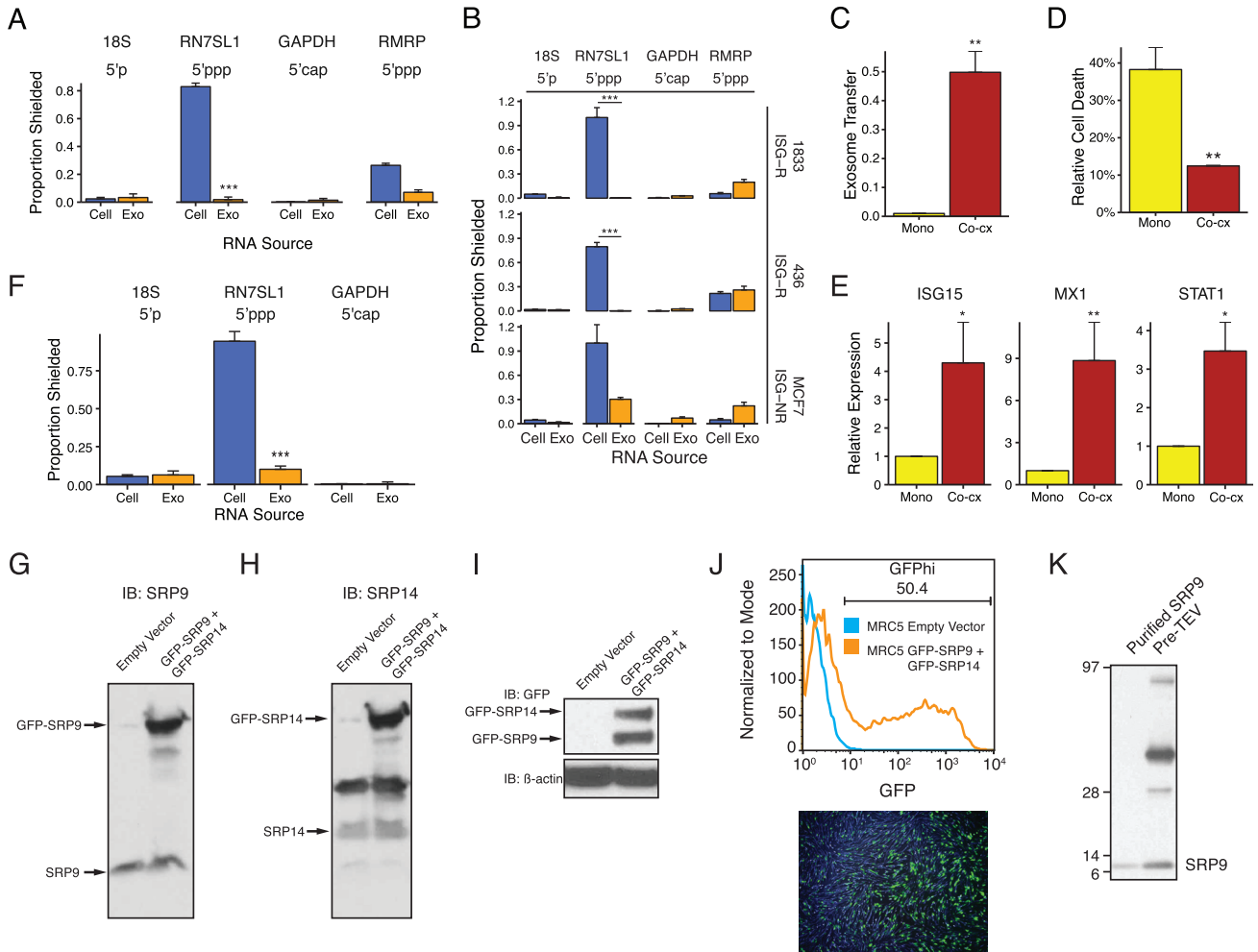


Figure S4. Differential RBP Shielding of RN7SL1 in Cells and Exosomes and Regulation by SRP9/14, Related to Figure 4

(A) Extent of RBP-shielding of 5'ppp RN7SL1 in cells (Cell) or exosomes (Exo) isolated from co-culture of 1833 and MRC5 cells. Proportion shielded is determined by MNase treatment with and without detergent followed by qRT-PCR (MNase-qRT-PCR) ($n = 3$). Also shown are other RNAs with the indicated 5' modification. (B) Extent of RBP-shielding for cellular RNA (Cell) or exoRNA (Exo) isolated from co-cultures of ISG-R or ISG-NR breast cancer cells (labeled on right margin) with MRC5 fibroblasts ($n = 3$). (C) Exosome transfer to ISG-R K14cre; p53^{F/F}; Brca1^{F/F} (KB1P) mouse breast cancer cells from other KB1P cells in mono-culture (Mono) or from primary mouse adult lung fibroblasts (ALFs) in co-culture (Co-cx). Exosome transfer was measured using differential lipid dye labeling ($n = 3$). (D) RT-mediated cell death in KB1P cells in mono-culture (Mono) or co-culture with ALFs (Co-cx). Cell death was assessed 4 days after 10 Gy RT ($n = 3$). (E) ISG expression in sorted KB1P cells after co-culture with ALFs. Gene expression values are relative to sorted KB1P cells grown in mono-culture ($n = 3$). (F) Extent of RBP-shielding of cellular RNA (Cell) or exoRNA (Exo) isolated from co-culture of KB1P cells and ALFs ($n = 3$). Immunoblot for (G) SRP9, (H) SRP14, or (I) GFP after transfection of GFP-SRP9 and GFP-SRP14 in MRC5 fibroblasts. (J) Flow cytometry (top) and fluorescence microscopy (bottom) for GFP expression after transfection of MRC5 stromal cells with GFP-SRP9 and GFP-SRP14. (K) Immunoblot for SRP9 pre-cleavage (lane 2) and post-cleavage (lane 1) of the GST tag with TEV protease. Error bars are SEM of biological replicates and * $p < 0.05$, ** $p < 0.01$, *** $p < 0.001$.

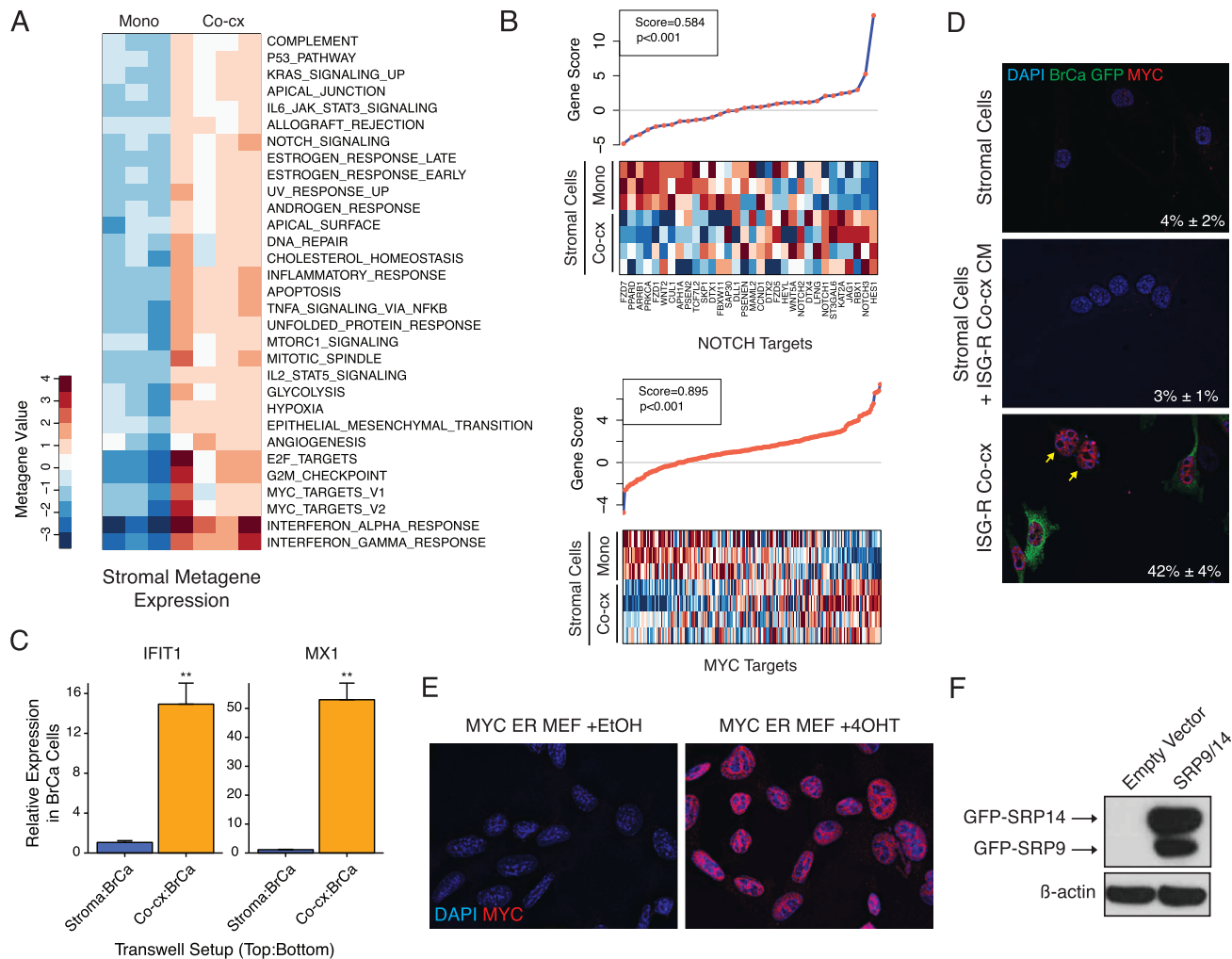


Figure S5. NOTCH and MYC Pathways Are Upregulated in Stromal Cells after ISG-R Co-culture, Related to Figure 5

(A) Heatmap showing metagene expression of significantly enriched hallmark gene sets in MRC5 fibroblasts after mono-culture (Mono) or co-culture with ISG-R breast cancer cells (Co-cx) as determined by gene set analysis. (B) Gene set analysis showing changes in NOTCH (top) and MYC (bottom) target genes in MRC5 fibroblasts after ISG-R co-culture compared to mono-culture. Top graph plots individual and overall gene scores, and bottom graph shows heatmap of expression of individual genes. (C) ISG expression in 1833 ISG-R breast cancer cells after using a transwell filter to separate 1833 cells from MRC5 fibroblasts (Stroma:BrCa) or from MRC5 fibroblasts co-cultured with 1833 cells (Co-cx:BrCa) ($n = 3$). Transwell filter pore size was large enough to allow exosome passage. (D) Immunofluorescence for MYC in MRC5 fibroblasts (top), MRC5 fibroblasts after addition of CM from ISG-R co-culture (middle), or in co-culture with 1833 ISG-R breast cancer cells (bottom). (E) Immunofluorescence for MYC in MYC-ER MEFs after treatment with 4OHT or vehicle control (+EtOH). (F) Immunoblot showing stable expression of GFP-SRP9 and GFP-SRP14 in MYC-ER MEFs. Error bars are SEM of biological replicates and $**p < 0.01$.

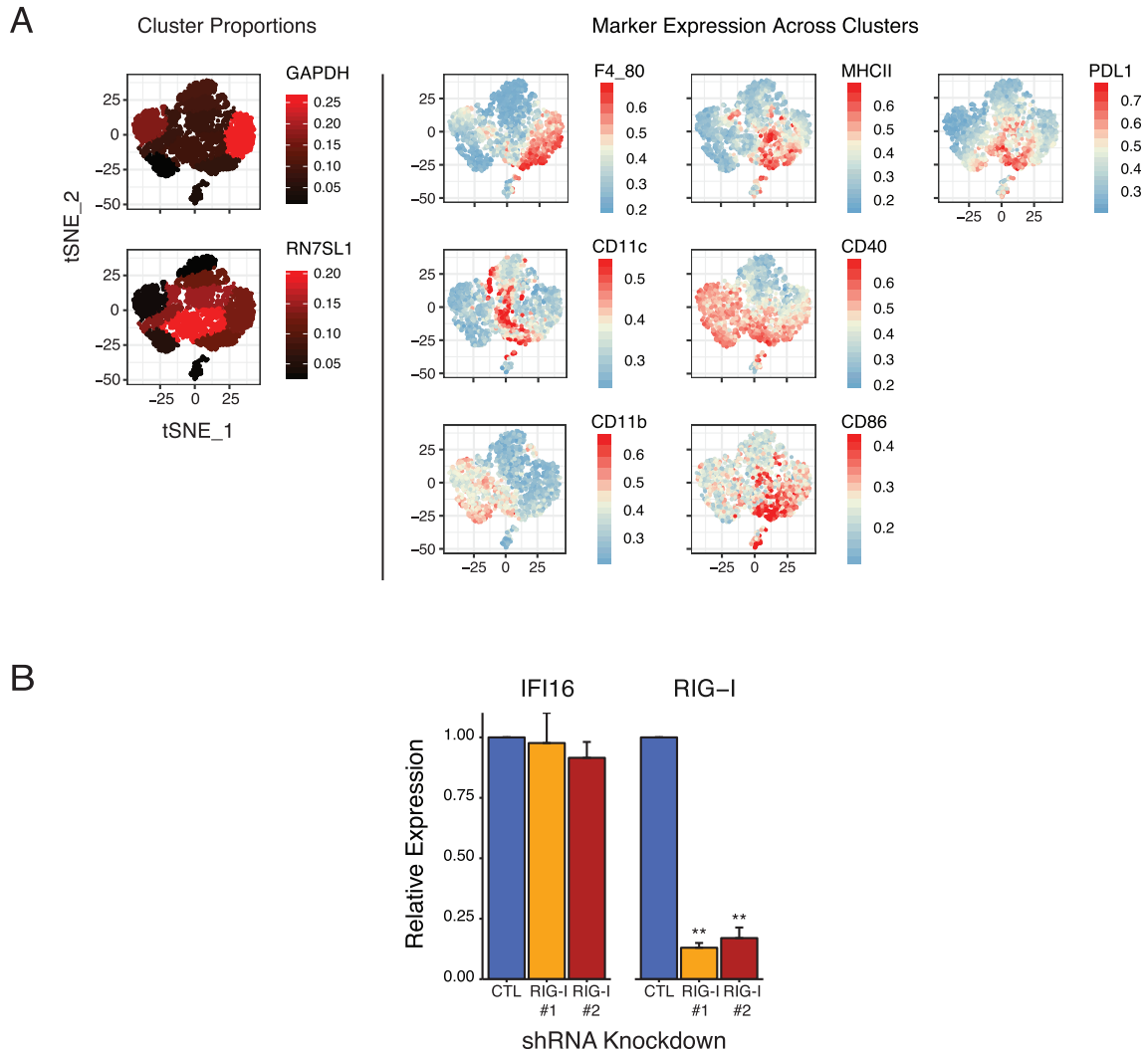


Figure S6. Unshielded *RN7SL1* Functions as a DAMP and Promotes Breast Cancer Progression, Related to Figure 6

(A) Unbiased flow cytometry analysis of splenic myeloid/DC populations using tSNE dimensionality reduction, cluster identification, and supervised classification. Representative data for mice injected with *RN7SL1* and GAPDH300 RNA encapsulated in liposomes. Shown are proportions of cells in each cluster as represented by the color gradient on the tSNE plot (left), which maps cells to a two-component dimensionality reduced space. Expression of the indicated markers is overlaid on the tSNE plot to visualize color-coded mean fluorescence intensities across clusters (right). (B) Gene expression in 4175 LM2 breast cancer cells after transduction of control shRNA (CTL) or two independent shRNAs to RIG-I (RIG-I #1 and RIG-I #2) ($n = 3$). *IFI16* is a control RNA not expected to change. Error bars are SEM of biological replicates and * $p < 0.01$.